

# Performance of preloaded and prestressed geosynthetic-reinforced soil

Taro Uchimura, Fumio Tatsuoka & Takeshi Sato

*Institute of Industrial Science (IIS), University of Tokyo, Japan*

Masaru Tateyama

*Japan Railway Technical Research Institute, Japan*

Yukihiko Tamura

*Tokyo Construction Co., Ltd, Japan*

**ABSTRACT:** A new construction method to make a reinforced soil structure very stiff and elastic is described. After a large vertical preload is applied, a large prestress is maintained using metallic tie rods which penetrate the reinforced soil vertically. Results from full-scale model tests and laboratory material tests to validate this method are described.

## 1 INTRODUCTION

Thirteen bridge abutments of geosynthetic-reinforced soil (GRS) retaining walls with a full-height rigid facing have been constructed for railways, while the longest bridge girder supported is 13.2 m (Tatsuoka et al., 1996b). For a more confident use for longer and heavier bridge girders, GRS bridge abutments must be more rigid. On the other hand, a GRS retaining wall with a full-height rigid facing located in one of the most seriously damaged areas during the 1995 Great Hanshin-Awaji earthquake did not fail at all, while some shear deformation with slight outward displacement and tilting of the facing was observed (Tatsuoka et al., 1996a). Increase in the shear rigidity of the backfill by increasing confining pressure is effective to restrain such shear deformations of GRS retaining wall.

In view of the above, a new construction method "preloaded and prestressed (PL • PS) reinforced soil" was developed (Fig. 1), which aims at making a reinforced soil structure very stiff (Tatsuoka et al., 1996c). To make a reinforced soil mass nearly elastic, large preload is applied by introducing tension into metallic tie rods which penetrate the reinforced soil and are fixed to the bottom reaction block. Being reinforced, the backfill soil can sustain large preload without failure. Tensile force  $T$  in the tie rods and the corresponding compressive load  $C$  in the backfill soil function as prestress to keep the confining pressure and soil stiffness high.

Compressive load  $P_c$  or tensile load  $P_t$  applied

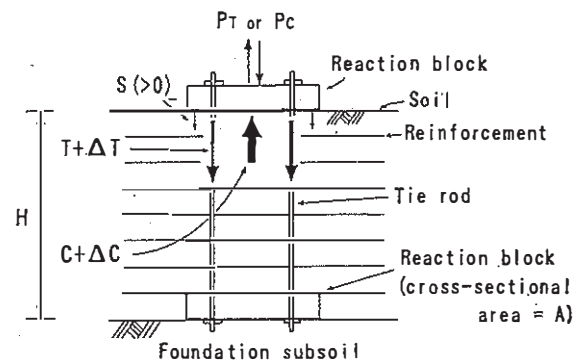


Fig. 1 PL • PS reinforced soil

to the top block is supported by both the tie rods in tension and the soil in compression. That is, when  $P_c$  is applied, the compression of the backfill decreases the tie rod tension by  $\Delta T$ , while the increase in the compressive load applied to the backfill is reduced to  $P_c - \Delta T$  from  $P_c$  when not prestressed. When  $P_t$  is applied, the elongation of the tie rods decreases the compressive force in the backfill by  $\Delta C$ , while the increase in the tie rod tension is reduced to  $P_t - \Delta C$  from  $P_t$  when not prestressed. Preloading also introduces a prestress in the reinforcement, which contributes to maintaining the integrity of the backfill soil.

To validate the above, full-scale test walls with gravel backfill were constructed at IIS Chiba.

Experiment Station, and viscous properties of the gravel, which control the relaxation rate of prestress, were investigated by triaxial tests.

## 2 FIELD FULL-SCALE MODEL TESTS

The test section (Figs. 2) is 5m-high, 7.4m-long, and 4.04m-wide, which is one of four test sections of a full-scale model test facility, separated by RC walls with a fixed distance. Segments 3S and 3N have the same configuration with a wrapped-around wall face constructed with a help of gabions filled with gravel. Full-height rigid facings have not been constructed. The central segment 3M is separated from 3S and 3N by 0.2m-thick unreinforced gravel zones. A well-graded crushed sandstone ( $D_{max} = 37.5\text{mm}$ ,  $D_{50} = 4\text{mm}$ ,  $U_c = 6.4\text{mm} / 0.09\text{mm} = 71$  and a fines content equal to 8.0%) was compacted to a dry density of  $1.88\text{g/cm}^3$  with an average water content of 7%. The grid made of polyvinyl

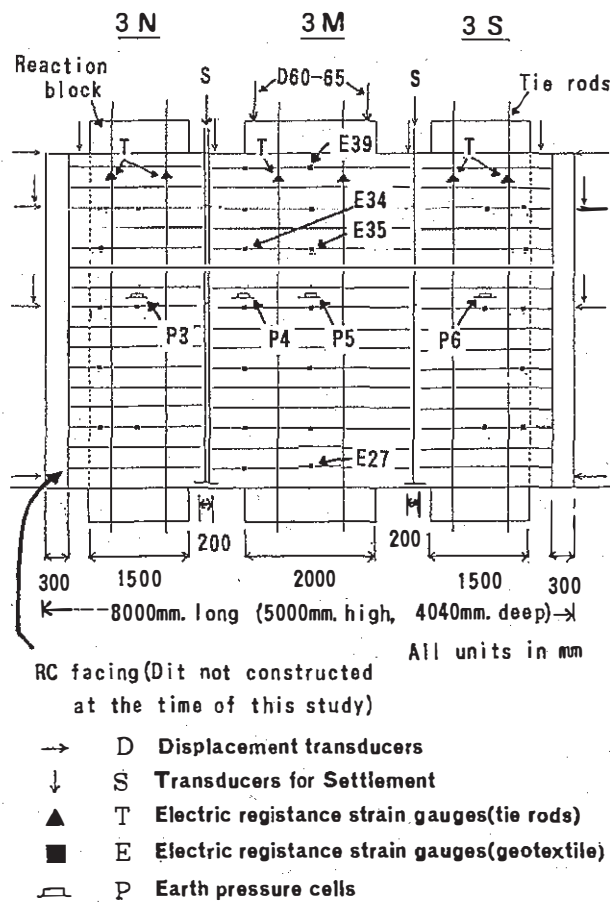


Fig. 2 a) Cross-section and b) the top view of the test section

alcohol (Vinyon) has a nominal tensile rupture strength  $73.5\text{kN/m}$  ( $7.5\text{tonf/m}$ ), which has been used to construct prototype GRS retaining walls. The weight of the each top RC block makes average contact pressure  $P_0 / (\text{contact area } A) = 11.8\text{kPa}$  ( $1.2\text{tonf/m}^2$ ). At the end of August 1995, Segment 3S was preloaded to  $(P_{PL} + P_0) / (A = 5.7\text{m}^2) = 133\text{kPa}$  ( $13.6\text{tonf/m}^2$ ) by introducing total tension  $P_{PL}$  in the four tie rods using four center-hole hydraulic jacks only for about 10 minutes (Fig. 3a). The increase in earth pressure ( $P_6$ ) due to  $P_{PL}$  measured at the center of the wall mid-height was very similar to the applied load (Fig. 4) (it was also the case with  $P_3$  in Segment 3N). Measured strains in the grid also

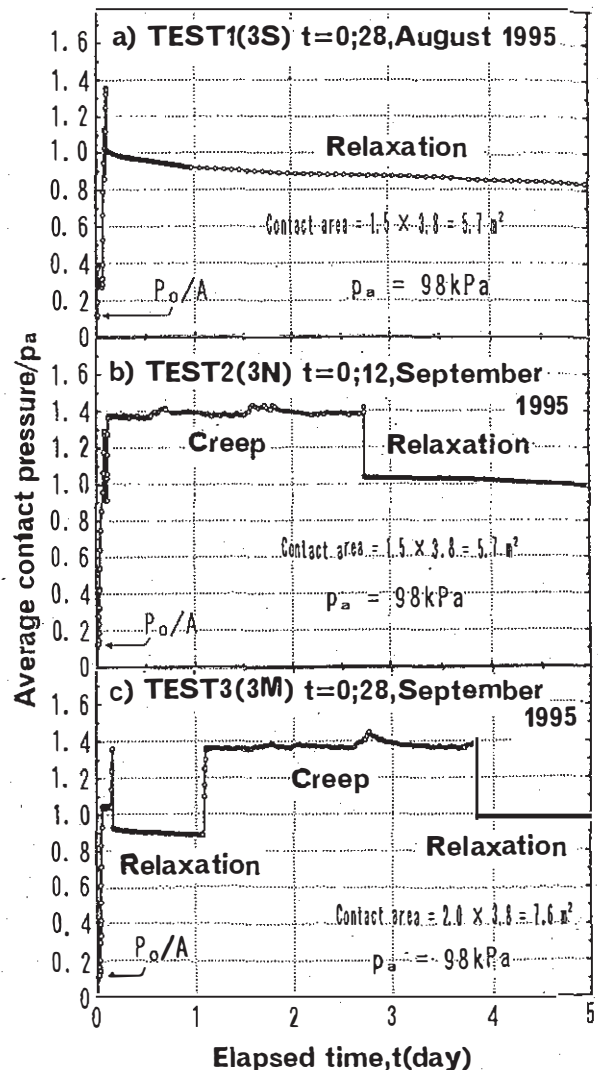


Fig. 3 Time histories of the average contact pressure  $(T + P_0)/A$  at the top RC block; a) 3S, b) 3N and c) 3M

showed that the backfill soil was loaded rather uniformly in the vertical direction. Next, the top ends of the tie rods were fixed to the top block, and the pressure in the hydraulic jacks were released. During that operation, the tie rod tension  $T$  dropped by about one - fourth of  $P_{PL}$ , probably due to inevitable slackness in the loading system. This drop in  $T$  was repeatable for the other segments. Then, the relaxation in the total tie rod tension  $T$  with time was monitored.

The test procedure for Segment 3N was similar except that creep deformation was allowed to occur for 63 hours at  $P_{PL}$  (Fig. 3b). Segment 3M was tested as follows. First some creep deformation was allowed for 2 hours at two-thirds of  $P_{PL}$ . Secondly, preload  $P_{PL}$  was applied, and then stress relaxation for 24 hours was observed. Next, preload  $P_{PL}$  was applied again for 72 hours. Then, the long-term observation of prestress was started.

Increment in the earth pressure below the edge

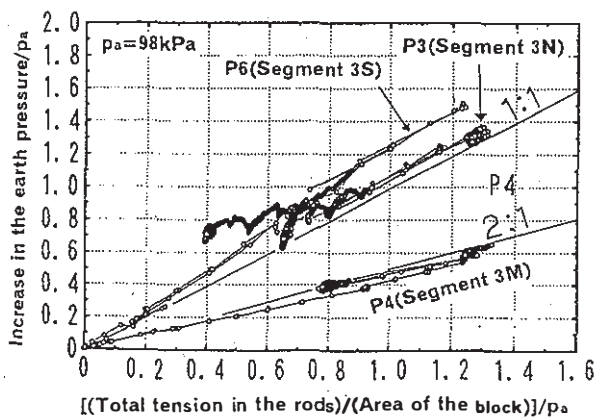


Fig. 4 Relationship between earth pressure increment and applied pressure  $T/A$

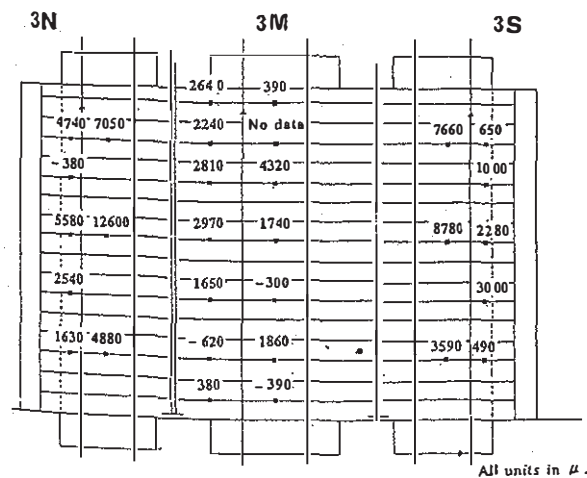


Fig. 5 Distribution of the grid tensile strains at the end of the last preloading

of the top block (P4) was about a half of the applied pressure (Fig. 4), which indicates a rapid change in the vertical pressure in the horizontal direction near the edges of the loaded area. The earth pressure cell (P5) at the center of the mid-height of 3M malfunctioned.

Grid strains at E34 and E35 responded very

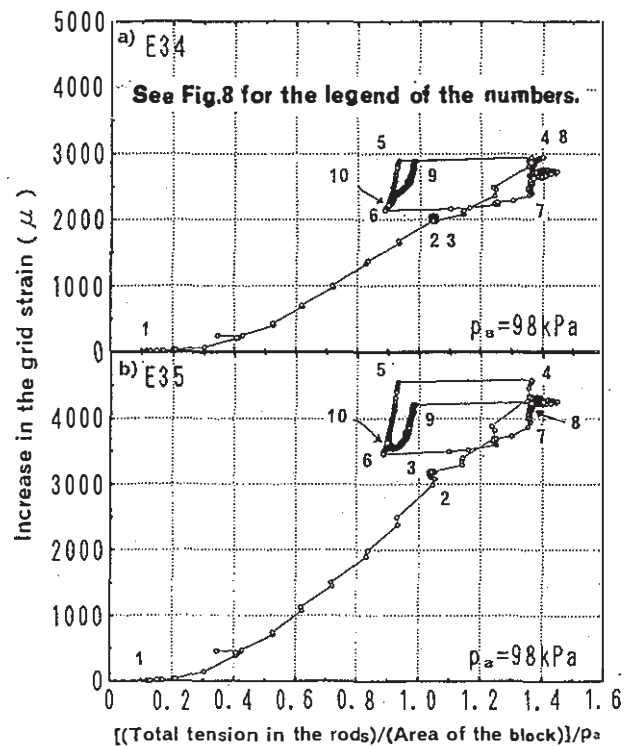


Fig. 6 Relationship between grid tensile strain increment and applied pressure  $T/A$  in Segment 3M; a) E34 and b) E35

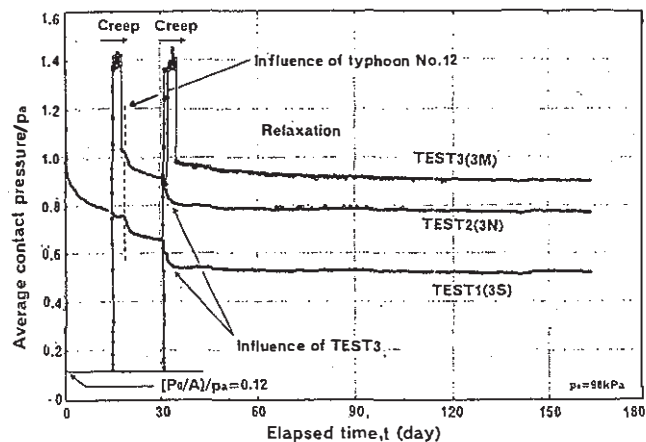


Fig. 7 Summary of the time histories of the average contact pressure  $(T + P_0)/A$  at the top RC block

well to applied load(Figs. 6a and 6b). Grid strains, however, scattered largely (Fig. 5). The following general trends may be seen from these data:

1. In Segment 3M, grid strains E27 and E39 in wedge zones immediately below the top blocks or immediately above the bottom blocks were small.
2. Grid strains are larger in the higher zones. One reason is vertical cracks appeared to some depth in the unreinforced zones between 3M, 3N and 3S. Another reason is possible stress concentration to the gabions in Segments 3N and 3S.

3. Grid strains are larger on the lines between centers of the top and bottom RC blocks than on the lines between the edges of them. That is, grid strains are largest at the center of the loaded areas.

Fig. 7 shows the summary of the time histories of the average contact pressure. Fig. 8 shows the average settlement plotted against the average contact pressure of the top RC block in Segment 3M. The following trends may be seen from these figures:

1. With creep deformation for very little period during preloading ( at 3S or the first one at 3M), the stress relaxation rate just after unloading was very high.
2. With relatively large creep deformation during preloading (at 3N or the second one at 3M), the stress relaxation rate just after unloading was very low.
3. Some amount of relaxation occurred by a total precipitation of more than 130mm by the Typhoon No.12 on 17th September 1995. As gravel had a fines content of 8% with an initial water content of about 7%, some suction should have been created during compaction. Part of

the suction may have been lost by wetting and small collapse -type compression may have occurred in the backfill to enhance stress relaxation.

4. When Segment 3M was preloaded, the tie rods tensions in Segments 3N and 3S reduced, perhaps due to the associated compression of the gravel in the segments.

5. After several weeks of relaxation, the relaxation rate became very low in all the segments. From 10th to 20th, December 1995, the average rate per day of Segments 3S, 3N and 3M were 0.034 kPa (0.0035 tonf/m<sup>2</sup>), 0.037 kPa (0.0038 tonf/m<sup>2</sup>) and 0.040 kPa (0.0041 tonf/m<sup>2</sup>), respectively.

6. The vertical stiffnesses of the walls during reloadings were much larger than those during the primary loadings (Fig. 8), which is the primary effect of preloading.

7. In Figs. 6a and b, grid tensile strains at point 5 was larger than those at point 3. This fact means that the reinforcement has been prestressed by the preloading.

8. Between points 5 and 6 and points 9 and 10, grid tensile strains (and tensile stresses) decreased during the relaxation stages. This is likely due to lateral creep compression of the backfill by the grid tensile stresses. The fact means the problem of outward creep deformation at the wall face, which has been one of the major concerns in the design of GRS retaining wall, are totally alleviated in PL + PS reinforced soil.

### 3 CREEP AND RELAXATION TESTS ON GRAVEL IN THE LABOLATORY

To explain the behaviour of the full-scale models described above and to know if the relaxation rate of prestress may be made small enough for a very long duration, the effects of preloading and associated creep deformation on the relaxation and creep properties at subsequent unloaded stages were investigated by triaxial tests (Fig. 9). The specimen was rectangular prism (57cm high and 23cm x 23cm in cross-section), made of the gravel used for the full-scale models having a water content of 6.9% and a dry density of 1.82g/cm<sup>3</sup>. Axial strain  $\epsilon_1$  and lateral strain  $\epsilon_3$  were measured locally with LDTs along the lateral surfaces of the specimen to remove the effects of bedding errors at the top and bottom ends and membrane penetration at the lateral surface(Goto et al.,1991). The specimen was consolidated isotropically to 49 kPa (0.5 kgf/cm<sup>2</sup>), and then deviator stress  $q$  was applied at a constant stress

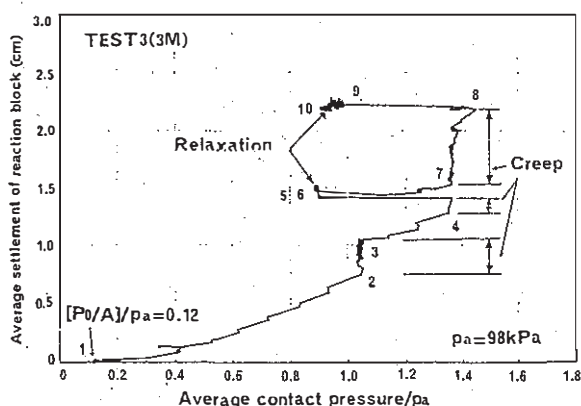


Fig. 8 Relationship between the average contact pressure  $(T+P_0)/A$  and the average settlement of the top RC block



rate  $dq/dt = 49 \text{ kPa/min}$  (Figs. 10a and b).

The test results are shown in Figs. 10 and 11. At several stages during primary loading and after unloading, either  $q$  was allowed to relax at constant  $\epsilon_1$  (relaxation stages R1 - R4) or  $\epsilon_1$  were allowed to increase at constant  $q$  (creep stages C1 - C8). The confining pressure was constant throughout the test ( $49 \text{ kPa} = 0.5 \text{ kgf/cm}^2$ ).

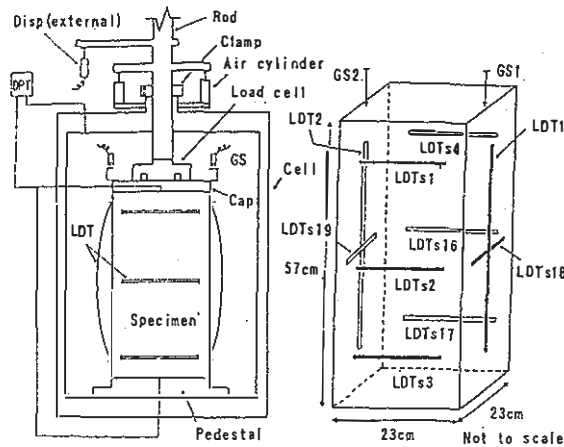


Fig. 9 Triaxial testing method using local displacement transducers LDTs

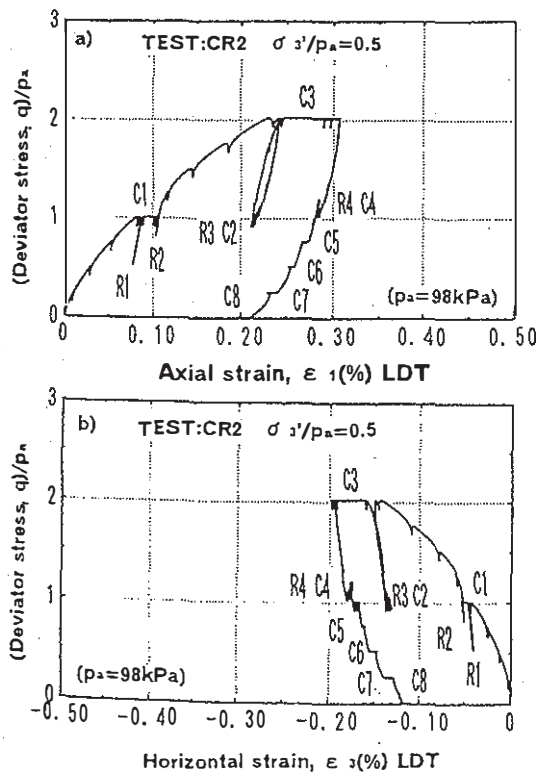


Fig. 10 Relationship between  $q$  and a)  $\epsilon_1$  and b)  $\epsilon_3$

The  $q$  values at Stages C1, C2 and C4 and the initial  $q$  values at Stages R1, R2, R3 and R4 were the same so as to examine solely the effects of preloading and associated creep deformation. At the relaxation stages, the local axial strain measured with LDTs elastically rebounded while the axial strain due to bedding error increased, especially at Stages R1 and R2 because the axial strain measured by external gauges (GS) (Fig. 9) was kept constant. Elastic properties measured by small unload / reload cycles are beyond the scope of this paper.

The following trends of behaviour are noted from Figs. 10 and 11:

1. The rates of stress relaxation and creep deformation are relatively large in the first relaxation/creep stages (R1 and C1).
2. The rates of relaxation/creep reduced largely by the first preloading (R3 and C2).
3. A trend of creep deformation and stress

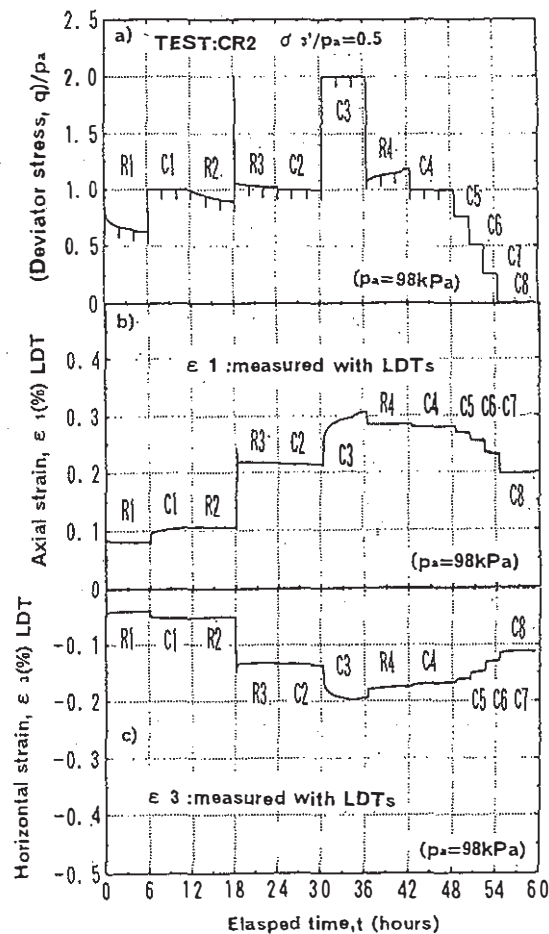


Fig. 11 Time histories of  $q$ ,  $\epsilon_1$  and  $\epsilon_3$

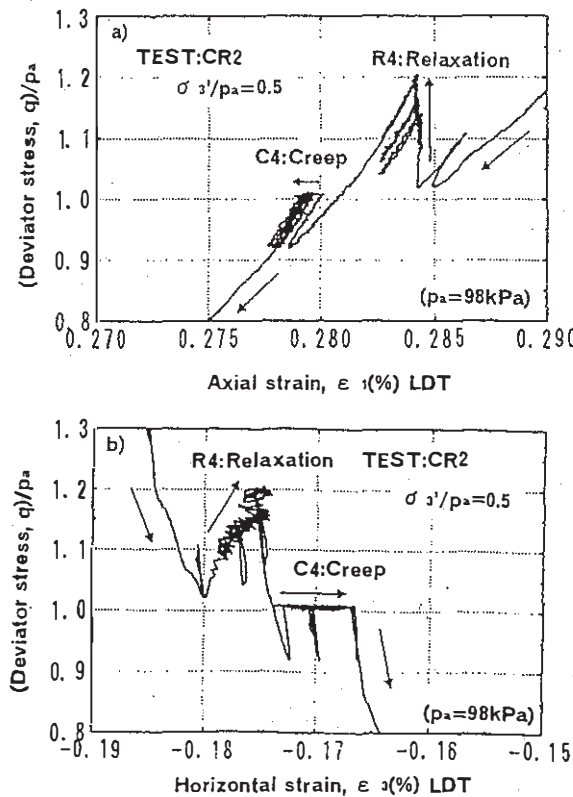


Fig. 12 Detailed result at Stages R4 and C4

relaxation totally disappeared after the second preloading, at which some creep deformation was allowed to occur. Rather, the compressive axial strain and the tensile lateral strain decreased with time at Stage C4, while the axial stress increased with time at stage R4 (Figs. 12a and b). Such "creep recovery" was observed also at Stages C5~C8 at lower stress levels. These behaviours can be explained by using a three-component rheological model having an elasto-plastic component connected to a pair of another elasto-plastic component and a dashpot in parallel.

The fact that the relaxation rate decrease largely by preloading is consistent well with the behaviours observed in the field tests. The triaxial test results also suggest that for field full-scale PL • PS reinforced soil, prestress may increase with time if a sufficient amount of creep deformation has been allowed to occur during preloading.

#### 4 CONCLUSIONS

The rigidity of a reinforced soil mass can be increased largely by proper preloading and prestressing. This point is supported by the

behaviour of the field full-scale models with highly-compacted well-graded gravel backfill with grid reinforcement. The relaxation rate of prestress can be made very small by allowing sufficient amount of creep deformation to occur during preloading, as supported also by the result of triaxial tests on the gravel. These results indicate that the application of this new construction method to actual construction project is quite feasible.

#### ACKNOWLEDGEMENTS

The authors are deeply indebted to their colleagues in helping us to perform this study, particularly Dr. Koseki, J., Dr. Kodaka, T., Mr. Muramoto, K., Mr. Motohiro, R., and Mr. Shibata, H. Valuable suggestions given by Prof. H. Di Benedetto, DGCE ENTPE, France, are gratefully acknowledged.

#### REFERENCE

- Goto, S., Tatsuoka, F., Shibuya, S., Kim, Y.-S. and Sato, T. (1991): A simple gauge for local small strain measurements in the laboratory, *Soils and Foundations*, 31-1, pp.169-180
- Tatsuoka, F., Tateyama, M., and Koseki, J. (1996a): Performance of soil retaining walls for railway embankments, Special Issue for the 1995 Great Hanshin Awaji earthquake, *Soils and Foundations*
- Tatsuoka, F., Tateyama, M., Koseki, J. and Uchimura, T. (1996b): Geotextile-reinforced soil retaining walls and their seismic behaviour, Special Lecture, Proc. of 10th Asian Regional Conf. on SMFE, 1995, Beijing, Vol. II (to appear)
- Tatsuoka, F., Uchimura, T. and Tateyama, M. (1996c): Preloaded and prestressed reinforced soil *Soils and Foundations* (submitted for review)